Introduction of numerical prediction methods for non-isothermal flows

Satoru Ushijima

Kyoto University, Japan

ushijima@media.kyoto-u.ac.jp

13th August 2014

Where am I from ?

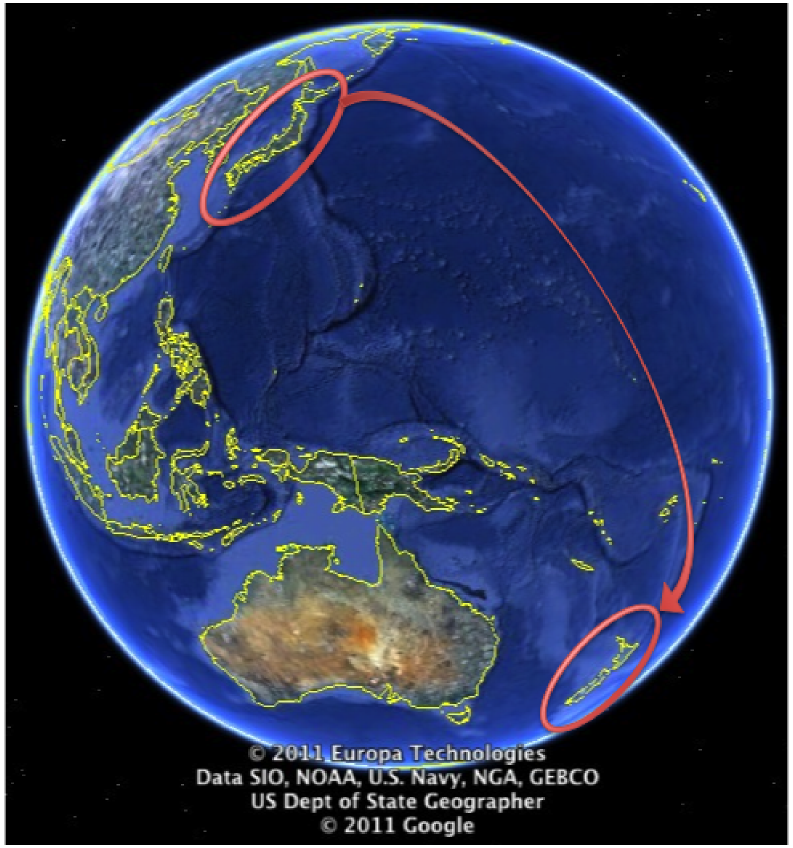

(a) Japan to New Zealand

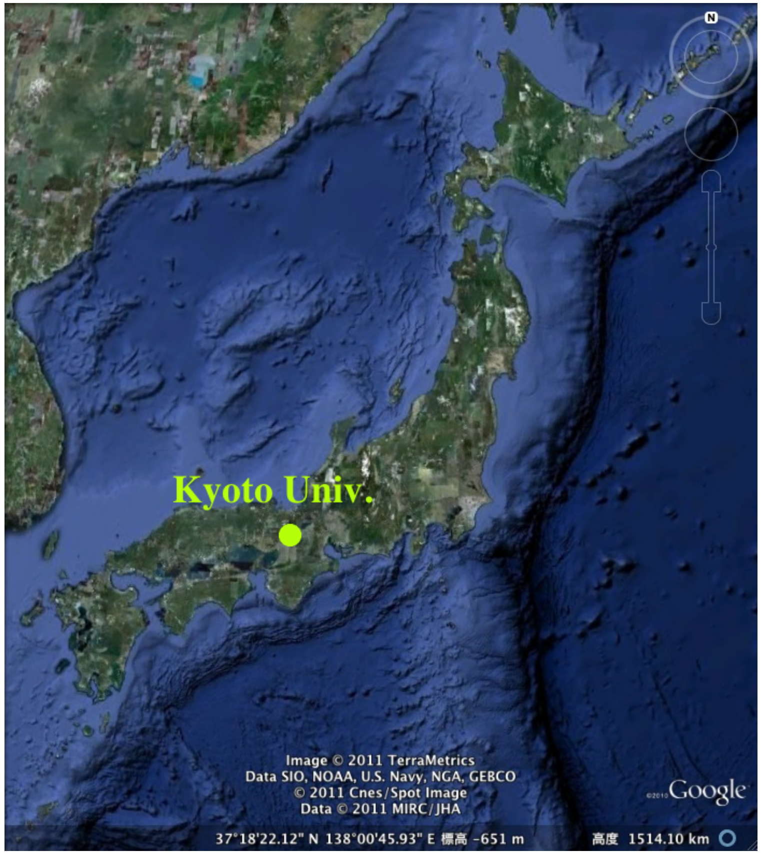

(b) Kyoto Univ. in Japan

8,800 km with 10-hour flight

Kyoto university

(a) Yoshida campus

(b) Katsura campus

- My Lab. is in ACCMS of Yoshida Main campus.
  ACCMS = Academic Center for Computing and Media Studies, where we deal with Supercomputers etc.
- The students in my Lab. (officially) belong to Civil and Earth Resources Eng. in Graduate School of Eng. in Katsura campus, located 15 km from Yoshida campus (actually stay in Yoshida).

Supercomputers in Kyoto Univ.

(a) SystemA(32Cores×940Nodes)

(b) SystemE(10+60Cores×482Nodes)

- ACCMS operates the Supercomputer in Kyoto Univ.
- Various types of Supercomputers (system A, B(G), C, D and E)
- Theoretical speed : 1.566 PFlops = $(1.566 \times 10^{15}$ Flops)
  $\approx 300.8 + 242.5 + 10.6 + 428.6 + 583.6$ (TF)

Some views near Yoshida campus

(a) Ginkaku-ji temple
= "Silver Pavilion" in English,
created in 1,490
(world heritage)

(b) Kamo river
Famous river in Kyoto city.
The riverbanks are popular
walks for residents and tourists.

Non-isothermal (or Density) flows

- Non-isothermal or density flows can be found near river mouths (salt wedge), thermal stratification in lakes and many other engineering fields.

(a) Salt wedge
(http://www.saltwedge.org/)

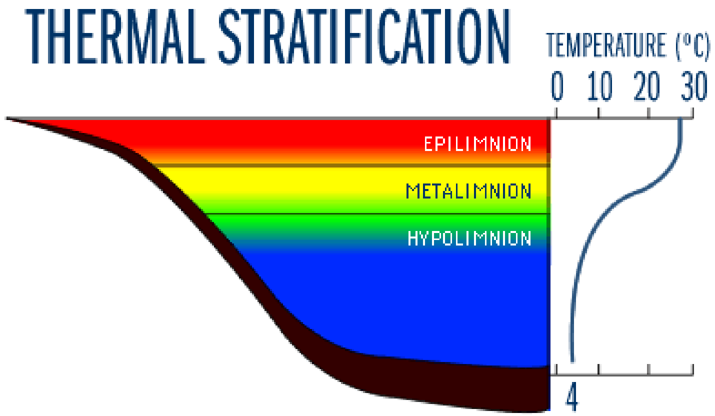

(b) Thermal stratification in lakes
(http://www.lakeaccess.org)

Lock-exchange problem

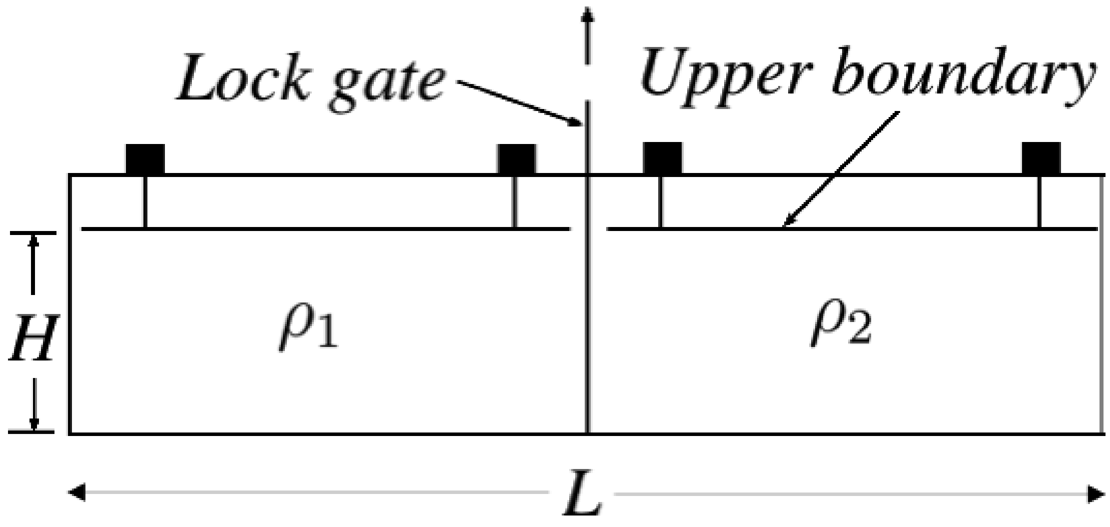

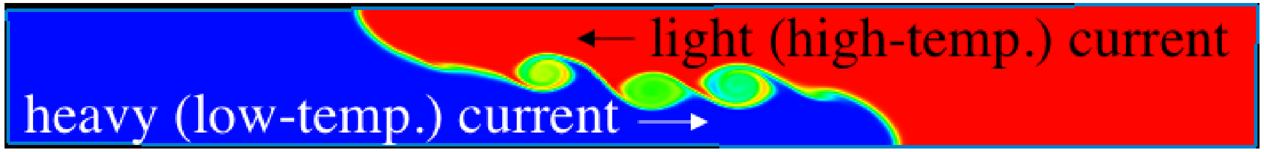

- $\rho_1 > \rho_2 \Rightarrow$ light and heavy currents arise
- Three numerical models are compared focusing on both front behaviors and conservation of mass in whole area.

Outline of today's topics

- Governing equations for density flows
- **Boussinesq approximations** for density flows
- Three models will be compared :

  model-A = Incompressible fluid model using
  all Boussinesq approximations

  model-B = Incompressible fluid model using
  partial Boussinesq approximations
  (not used BA for momentum eqs.)

  model-C = Compressible fluid model
  (using no approximations)

Classical laws for fluids and governing eqs.

- Mass conservation law
- Newton's second law of motion
- First law of thermodynamics
- Relation between state variables (e.g. $p \leftrightarrow \rho, e$)

$$\Downarrow$$

- Mass conservation equation (1 eq. : $\rho, \boldsymbol{u}$)
- Momentum equations (3 eqs. in 3D space : $\rho, \boldsymbol{u}, p$)
- Energy equation (1 eq. : $e, \rho, \boldsymbol{u}, p$)
- Equation of state (1 eq. : p, ρ, e)

Fluid variables in Control Volume (CV)

- Descriptions of fluid variables : L and E
  Eulerian description : $\rho(t, \boldsymbol{x})$
  (independent variables = t and $\boldsymbol{x}$ fixed in space)

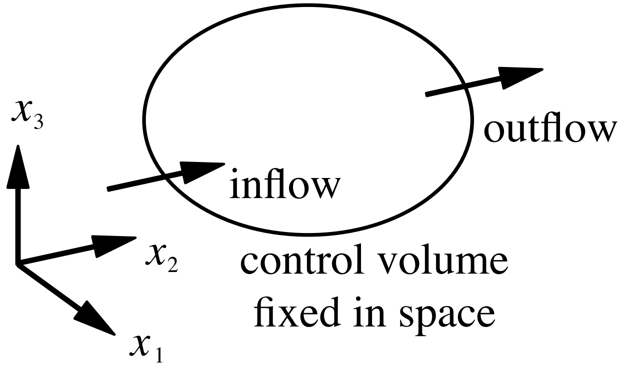

- Consider conservation laws in the Control Volume (CV) that is fixed in space and its surface always keeps same shape.

Mass conservation in CV

- Increase rate of mass in CV = Incoming mass into CV

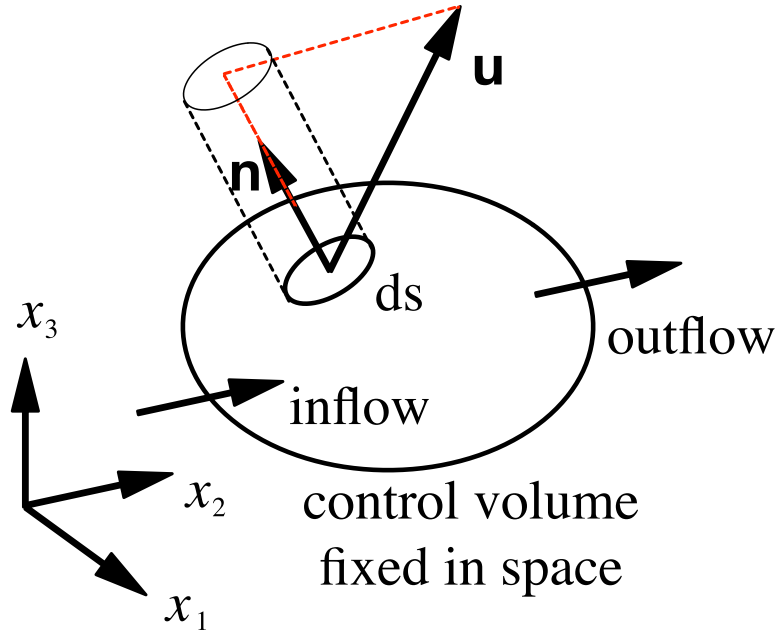

$$\frac{\partial}{\partial t}\int_V \rho \, dv = -\int_S \rho u_i n_i \, ds \quad \text{(integral form)}$$

- where $\boldsymbol{n}$ is outward normal unit vector on CV surface

Mass conservation in CV (cont.)

- Gauss' divergence theorem :

$$\int_V \nabla \boldsymbol{A} \, dv = \int_S \boldsymbol{A} \cdot \boldsymbol{n} \, ds$$

or when $\boldsymbol{A} = (a_1, a_2, a_3)$, it is same as

$$\int_V \frac{\partial a_i}{\partial x_i} \, dv = \int_S a_i n_i \, ds$$

Thus, the integral form of mass conservation becomes

$$\frac{\partial \rho}{\partial t} + \frac{\partial (\rho u_i)}{\partial x_i} = 0 \tag{1}$$

Governing eqs. for compressible fluid

- Similarly, we derive the other eqs.
- Momentum eqs. for Newtonian fluid :

$$\rho \frac{\partial u_i}{\partial t} + \rho \frac{\partial (u_i u_j)}{\partial x_j} = \rho g_i - \frac{\partial p}{\partial x_i} + \mu \frac{\partial^2 u_i}{\partial x_j^2} \qquad (2)$$

- Eq. for temperature ($\alpha_T =$ thermal diffusivity) :

$$\frac{\partial T}{\partial t} + \frac{\partial (T u_j)}{\partial x_j} = \frac{Q}{c_v \rho} + \alpha_T \frac{\partial^2 T}{\partial x_j^2} \qquad (3)$$

- Eq. of state (ideal gas) : $p = c_v(\gamma - 1)\rho T$ (4)

  where $\gamma = c_p/c_v$, c_p and c_v are specific heats at constant pressure and volume, respectively.

Model-C

- With eqs. (1) to (4), we can predict compressible (and incompressible) fluids with no approximations.
- **Model-C** : consists of all eqs. (1) to (4)

Boussinesq approximations

- Simple relationship between ρ and T :

$$\rho = \frac{\rho_0}{1 + \beta(T - T_0)} \qquad (\rho_0 = \text{const. at } T = T_0)$$

where β = coefficient of thermal expansion.

- When $\beta(T - T_0) \ll 1$, we have

$$\rho = \frac{\rho_0}{1 + \beta(T - T_0)} \approx \rho_0[1 - \beta(T - T_0)] \equiv \rho_0 + \Delta\rho$$

- **Boussinesq approximations (BA) :**
  (a) neglect $\Delta\rho$ in mass conservation eq.
  (b) neglect $\Delta\rho$ only on LHS of momentum eqs.

Mass conservation eq. with BA (a)

- Original mass conservation eq.

$$\frac{\partial \rho}{\partial t} + \frac{\partial (\rho u_i)}{\partial x_i} = 0$$

- With BA (a), mass conservation becomes

$$\frac{\partial (\rho_0 + \cancel{\Delta \rho})}{\partial t} + \frac{\partial [(\rho_0 + \cancel{\Delta \rho}) u_i]}{\partial x_i} = 0 \quad \rightarrow \quad \frac{\partial u_i}{\partial x_i} = \nabla \boldsymbol{u} = 0$$

- $\nabla \boldsymbol{u} = 0$ means the incompressible condition, as a result, the fluid becomes "incompressible".

Model-B

- **Model-B** uses only BA (a).
- incompressible fluid : $\nabla \boldsymbol{u} = 0$
- Momentum eqs. :

$$\rho \frac{\partial u_i}{\partial t} + \rho \frac{\partial (u_i u_j)}{\partial x_j} = \rho g_i - \frac{\partial p}{\partial x_i} + \mu \frac{\partial^2 u_i}{\partial x_j^2}$$

- Eq. for temperature :

$$\frac{\partial T}{\partial t} + \frac{\partial (T u_j)}{\partial x_j} = \frac{Q}{c_v \rho} + \alpha_T \frac{\partial^2 T}{\partial x_j^2}$$

- Relationship for ρ and T : $\rho = \rho_0 / [1 + \beta (T - T_0)]$

Momentum eqs. with BA (b)

- With BA (b) in addition to BA (a), momentum eqs. become

$$\rho\frac{\partial u_i}{\partial t} + \rho\frac{\partial (u_i u_j)}{\partial x_j} = \rho g_i - \frac{\partial p}{\partial x_i} + \mu\frac{\partial^2 u_i}{\partial x_j^2}$$

$$\Downarrow$$

$$(\rho_0 + \cancelto{}{\Delta\rho})\frac{\partial u_i}{\partial t} + (\rho_0 + \cancelto{}{\Delta\rho})\frac{\partial (u_i u_j)}{\partial x_j} = \rho g_i - \frac{\partial p}{\partial x_i} + \mu\frac{\partial^2 u_i}{\partial x_j^2}$$

$$\Downarrow \quad \times 1/\rho_0$$

$$\frac{\partial u_i}{\partial t} + \frac{\partial (u_i u_j)}{\partial x_j} = \frac{\rho}{\rho_0} g_i - \frac{1}{\rho_0}\frac{\partial p}{\partial x_i} + \nu\frac{\partial^2 u_i}{\partial x_j^2}$$

Model-A

- **Model-A** uses BA (a) and (b).
- incompressible fluid : $\nabla \boldsymbol{u} = 0$
- Momentum eqs. :

$$\frac{\partial u_i}{\partial t} + \frac{\partial (u_i u_j)}{\partial x_j} = \frac{\rho}{\rho_0} g_i - \frac{1}{\rho_0}\frac{\partial p}{\partial x_i} + \nu \frac{\partial^2 u_i}{\partial x_j^2}$$

- Eq. for temperature :

$$\frac{\partial T}{\partial t} + \frac{\partial (T u_j)}{\partial x_j} = \frac{Q}{c_v \rho} + \alpha_T \frac{\partial^2 T}{\partial x_j^2}$$

- Relationship for ρ and T : $\rho = \rho_0 / [1 + \beta (T - T_0)]$

Summary of three Models

- Three numerical models are summarized as

model	BA (a)	BA (b)	fluid
model-A	Yes	Yes	Incompressible
model-B	Yes	No	Incompressible
model-C	No	No	Compressible

- Next, we will compare three models
  using experimental results of lock-exchange problems.

Experiments (R.J.Lowe, et al., 2005)

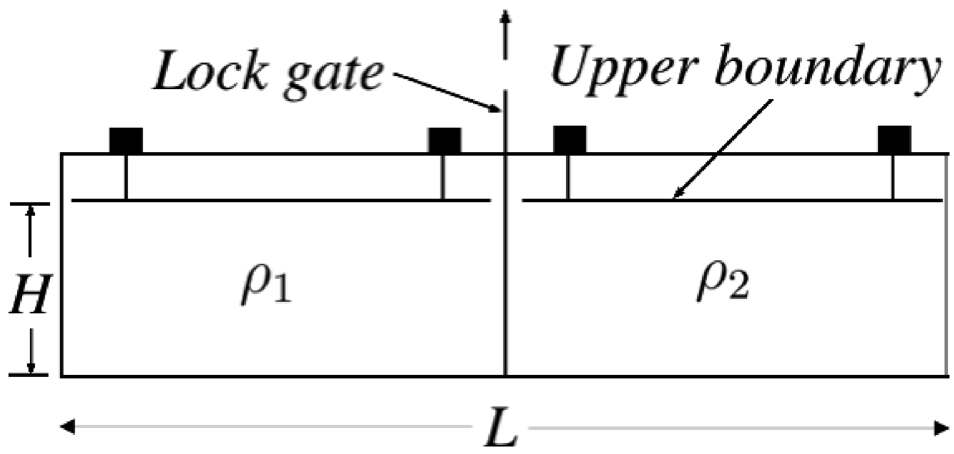

- $H = 0.2$ m, $L = 1.82$ m
- Density ratio : $r = \rho_2/\rho_1 < 1$ (since $\rho_2 < \rho_1$)
- Targets : $r = 0.993$ and $r = 0.681$
- non-dim. time : $t^* \equiv t\sqrt{g(1-r)/H}$

Conditions of computations

- Finite Volume Method and accurate schemes originally developed in our Lab.
- Non-slip and adiabatic conditions for all boundaries
- 256 parallel computations using system-A in Kyoto University supercomputer with flat MPI

Front shapes ($r = 0.993$)

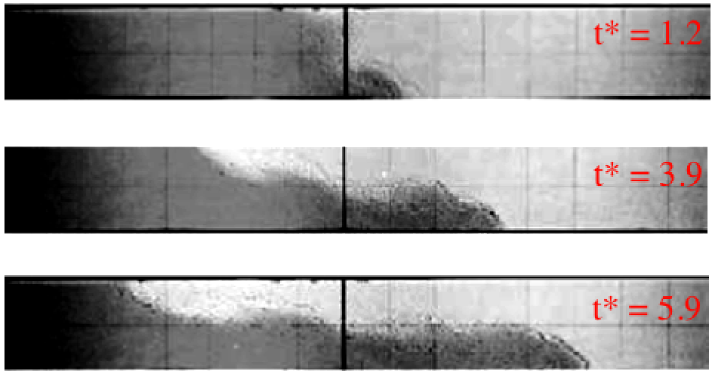

(a) exp. (R.J.Lowe, et al., 2005)

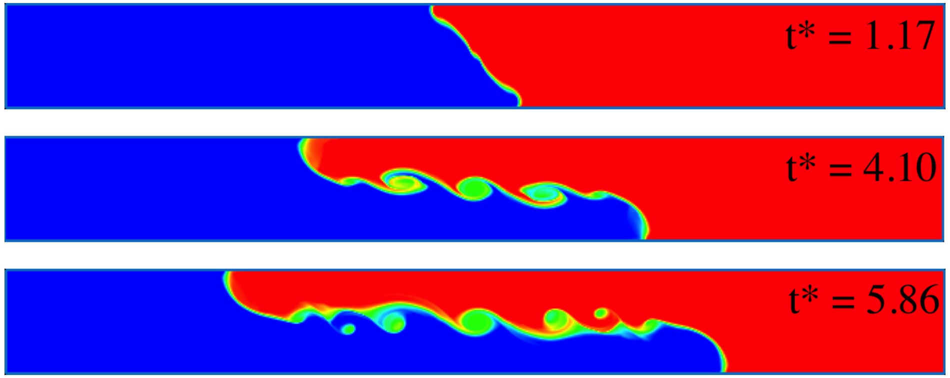

(b) **model-A**

- Predicted results by **model-A** are shown on the right side.

Front shapes ($r = 0.993$)

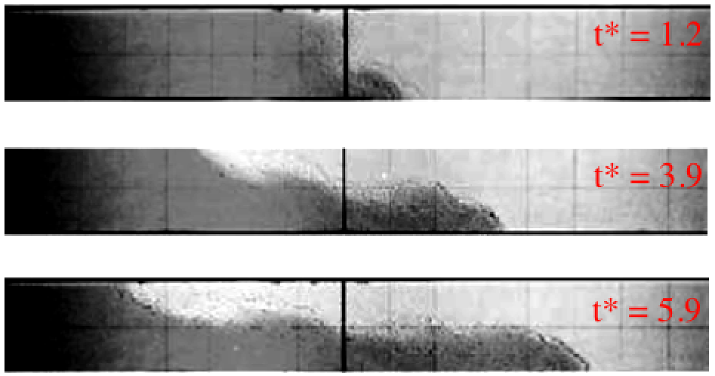

(a) exp. (R.J.Lowe, et al., 2005)

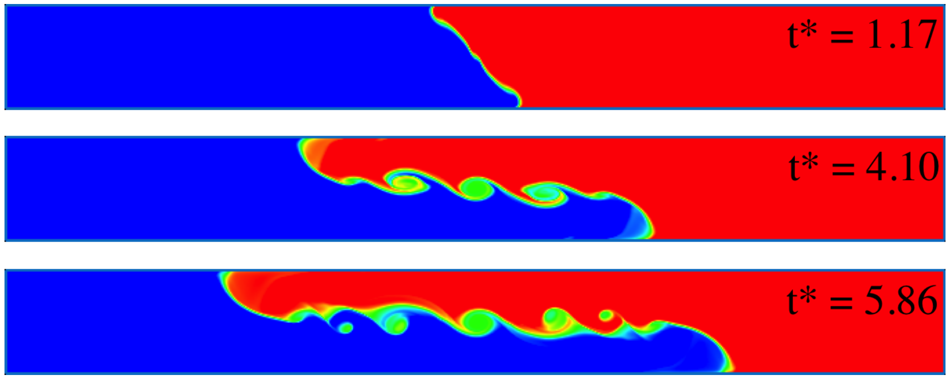

(b) **model-B**

- Predicted results by **model-B** are shown on the right side.

Front shapes ($r = 0.993$)

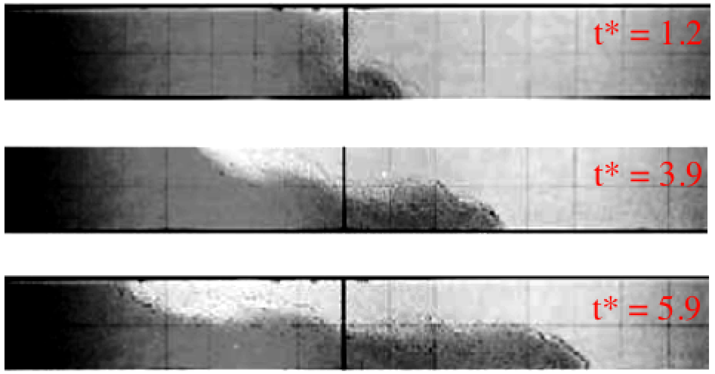

(a) exp. (R.J.Lowe, et al., 2005)

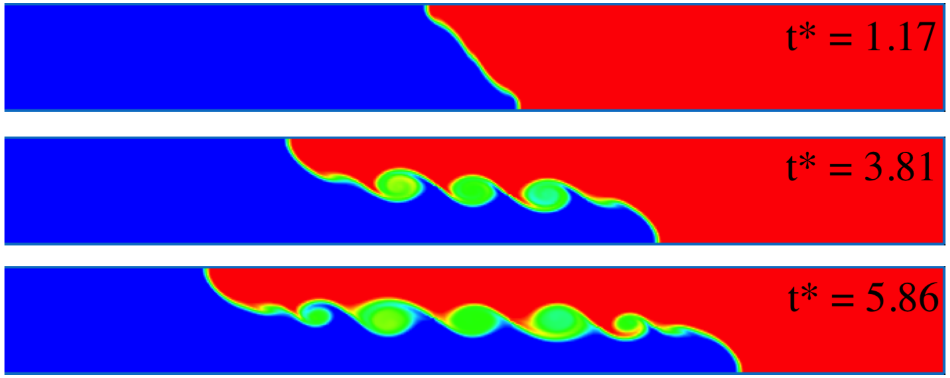

(b) **model-C**

- Predicted results by **model-C** are shown on the right side.

Front shapes ($r = 0.681$)

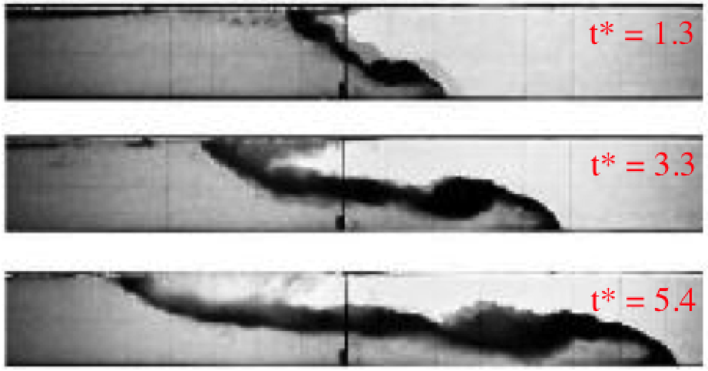

(a) exp. (R.J.Lowe, et al., 2005)

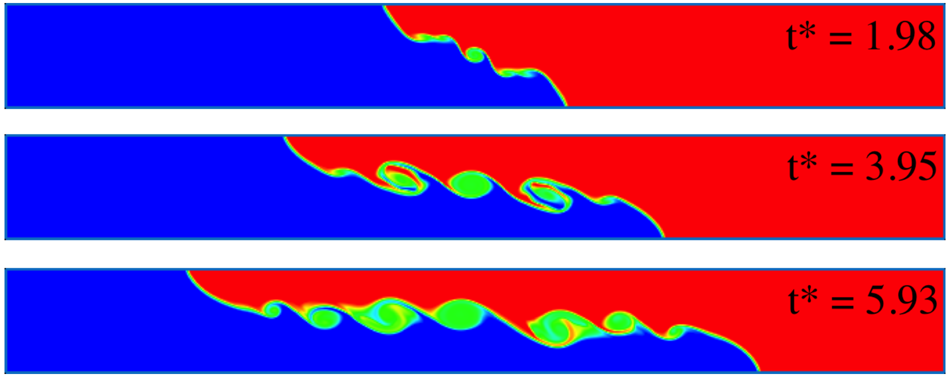

(b) **model-A**

- Predicted results by **model-A** are shown on the right side.

Front shapes ($r = 0.681$)

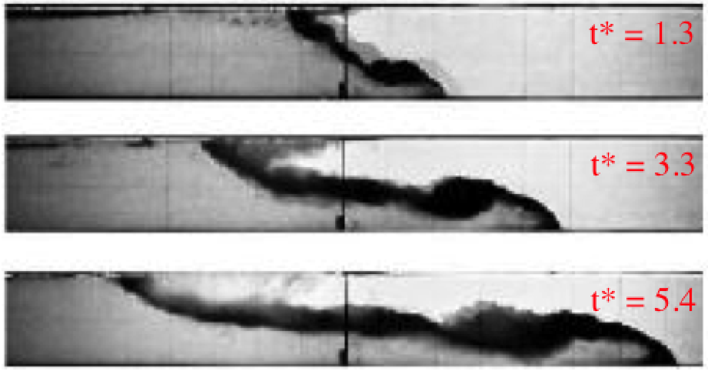

(a) exp. (R.J.Lowe, et al., 2005)

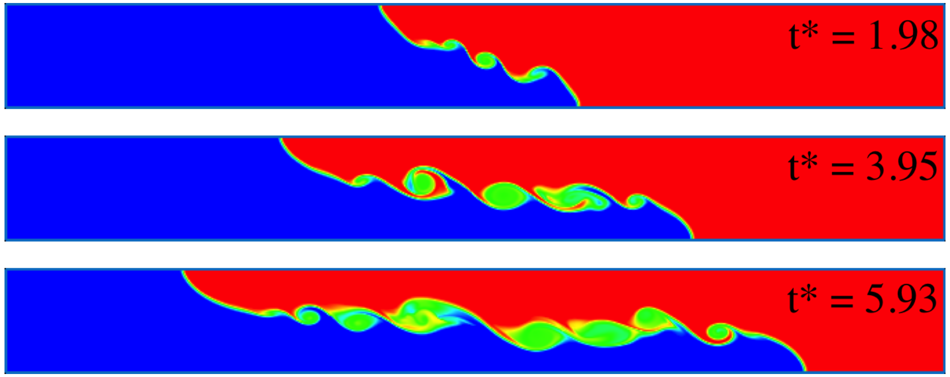

(b) **model-B**

- Predicted results by **model-B** are shown on the right side.

Front shapes ($r = 0.681$)

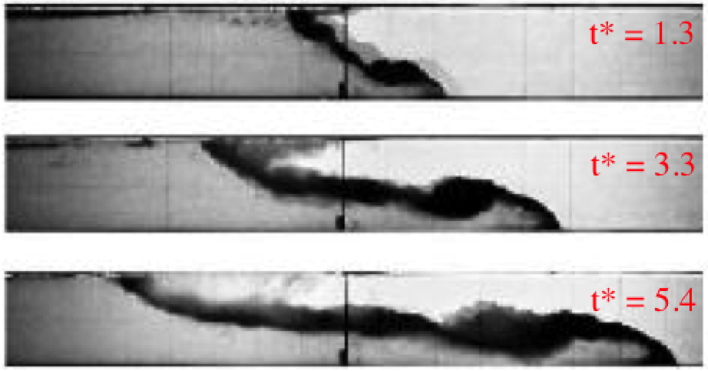

(a) exp. (R.J.Lowe, et al., 2005)

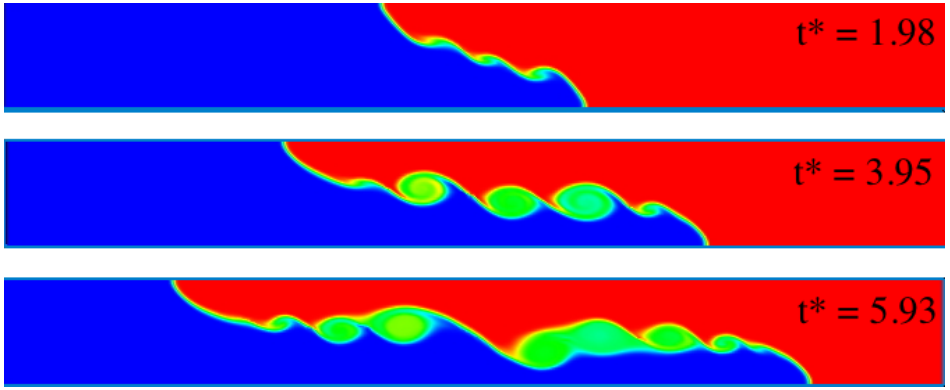

(b) **model-C**

- Predicted results by **model-C** are shown on the right side.

Front positions (R.J.Lowe, et al., 2005)

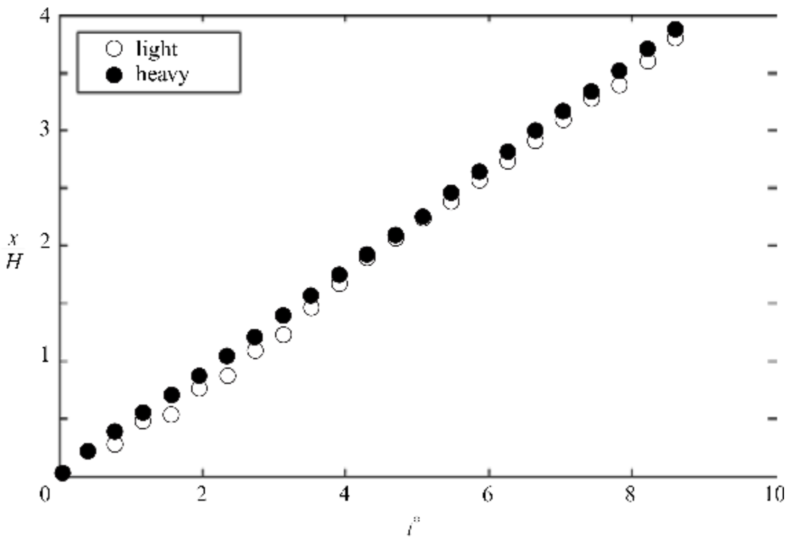

(a) $r = 0.993$

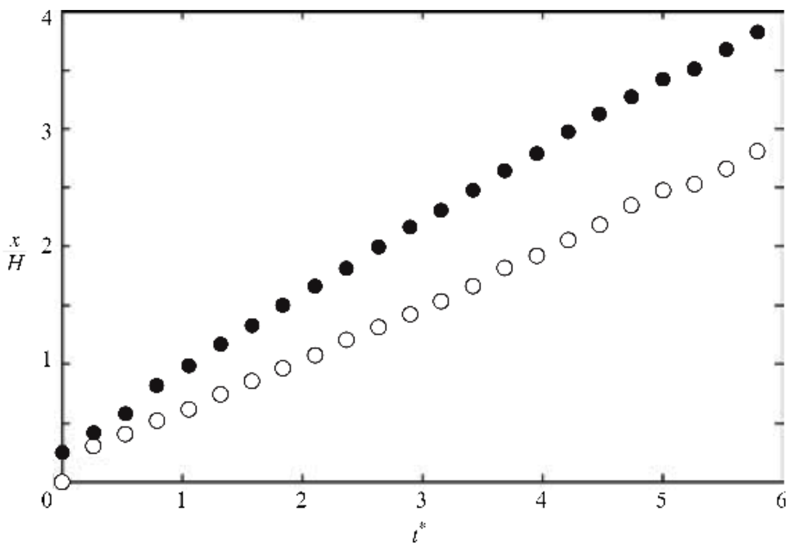

(b) $r = 0.681$

- $r = 0.993$: Heavy (●) and light fronts (○) are almost same
- $r = 0.681$: Heavy front (●) moves faster than light front (○)

Predicted Front positions : model-A

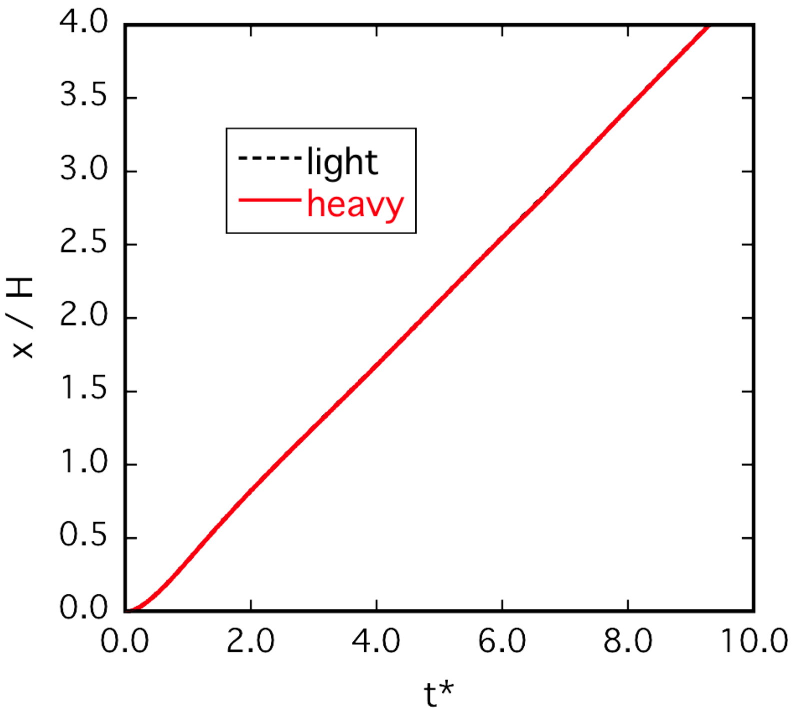

(a) $r = 0.993$

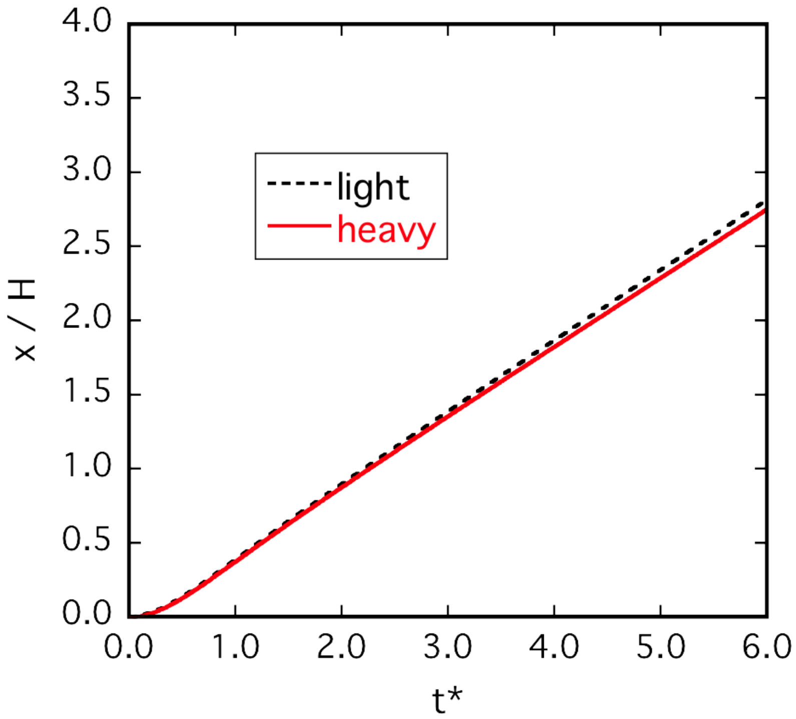

(b) $r = 0.681$

- **model-A** cannot predict the differences between light and heavy front positions in (b) $r = 0.681$.

Predicted Front positions : model-B

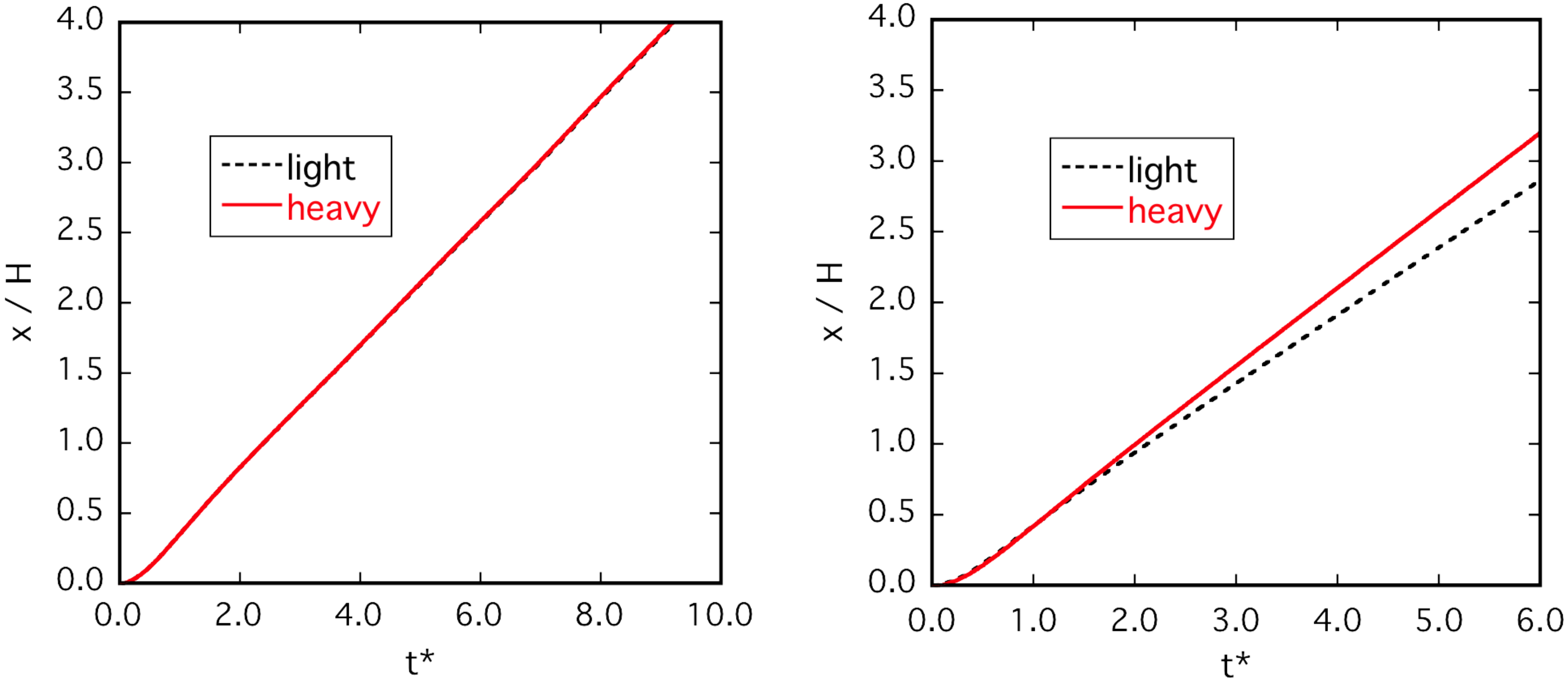

(a) $r = 0.993$ (b) $r = 0.681$

- **model-B** can predict the differences qualitatively between light and heavy front positions in (b) $r = 0.681$.

Predicted Front positions : model-C

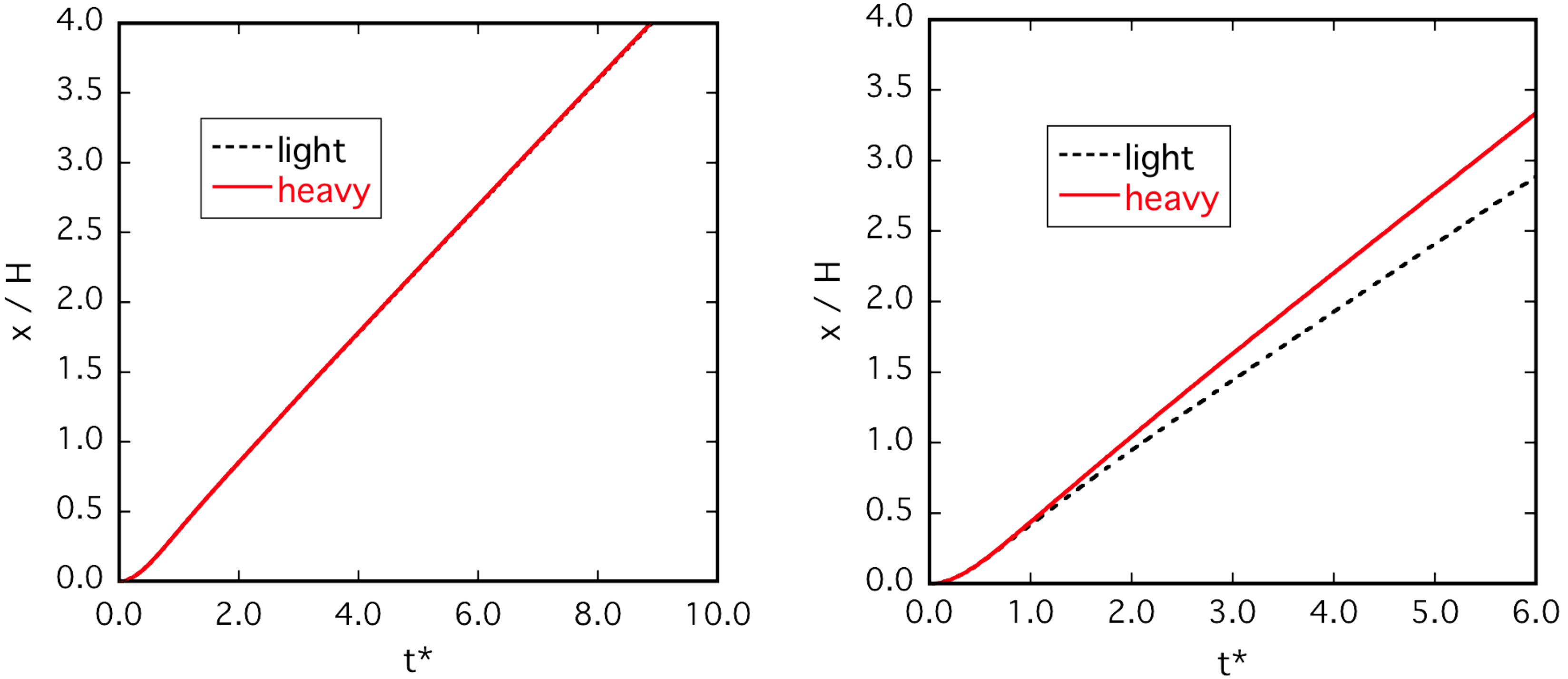

(a) $r = 0.993$ (b) $r = 0.681$

- **model-C** can also predict the differences qualitatively between light and heavy front positions in (b) $r = 0.681$.

Mass conservation (calculations)

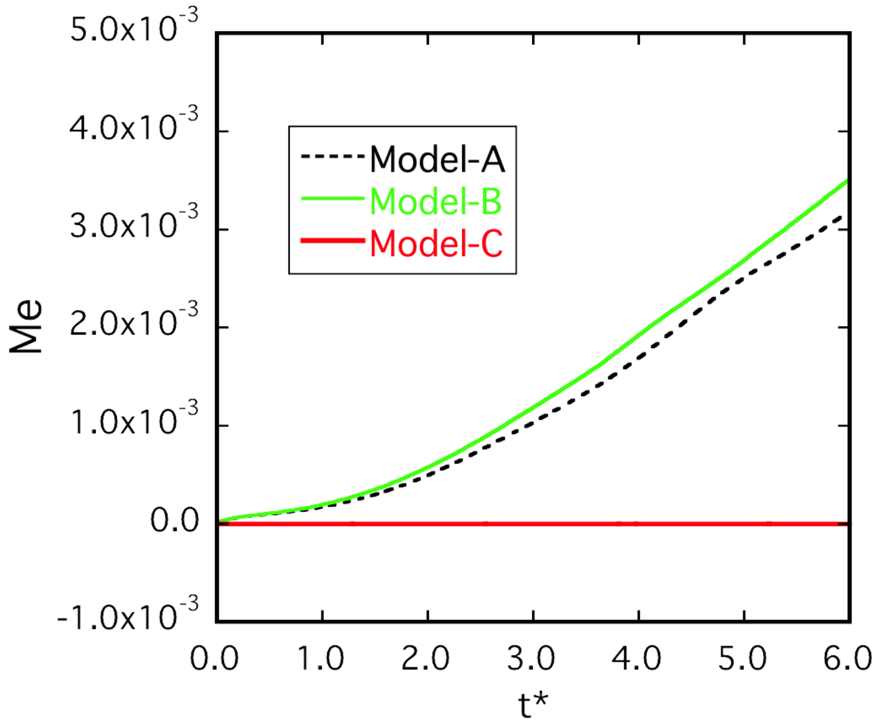

- M_e is non-dim. error of mass conservation. $M_e = |M - M_0|/M_0$, where M and M_0 are mass of whole area at $t = t$ and 0.
- M_e should be 0 and **model-C** gives the best results.

Computational time

- Computational time in case of $r = 0.681$
- 256 parallel computations with flat MPI

model	Δt	grid num.	CPU time per 1 sec.
model-A	1.0×10^{-3}	2,725,888	7.77 min.
model-B	1.0×10^{-3}	2,725,888	7.88 min.
model-C	5.0×10^{-6}	340,736	1.53 hours

- **model-C** needs large CPU time, although number of computational grid points is small.

Concluding remarks

1) When density ratio ≈ 1, front positions are reasonably predicted by ALL models.

2) However, when density ratio is small (≤ 0.7), **model-A** cannot predict front positions accurately, while **model-B** and **model-C** can do it.

3) Regarding mass conservation, **model-A** and **model-B** have slight errors, while **model-C** is perfect.

4) **model-C** needs large computational time.

5) Conclusively, **model-B** may be practically useful.